

## **CHAPTER-4**

---

---

**In vitro bioactivity and mechanical  
properties of zirconium dioxide  
doped 1393 bioactive glass**

---

---



### 4.1 Introduction

The first bioactive glass used as a bioactive material was 45S5 bioactive glass which has four-component silica glass (45 wt% SiO<sub>2</sub>, 24.5 wt% CaO, 24.5 wt% Na<sub>2</sub>O and 6 wt% P<sub>2</sub>O<sub>5</sub>) [Hench et al., 2006]. In the 45S5 bioactive glass, S denotes the network former SiO<sub>2</sub> followed by a specific Ca/P molar ratio of 5:1 [M. Best, A.E.Porter, E.S.Thian, and J. Huang, 2008]. The key compositional features that are accountable for the bioactivity of Hench bioactive glass are its low SiO<sub>2</sub>, high Na<sub>2</sub>O, and CaO contents as well as high CaO/P<sub>2</sub>O<sub>5</sub> relative amount [M.N.Rahaman, D.E.Day, B.S.Bal, Q.Fu, S.B.Jung, 2011 and Ankesh Kumar Srivastava, Ram Pyare and S. P. Singh, 2012]. One more silicate-based bioactive glass, designated as 1393, with a customized 45S5 bioactive glass composition [Brink M. et al.,1997], has easier viscous flow behavior and less tendency to crystallize than 45S5 bioactive glass. The 1393 glass is approved for in vivo use in Europe [Qiang Fu, Mohamed N. Rahaman, B. Sonny Bal, Roger F. Brown, Delbert E. Day, 2008]. However, this bioactive glass was lean from mechanical weakness and low fracture toughness due to the amorphous nature of glass, and therefore, it may not be appropriate for load-bearing applications [D. Shi Ed, Biomaterials, 2006]. Bio inert (zirconia, alumina), bioactive (hydroxyapatite, bioactive glasses, and glass-ceramics), resorbable (tricalcium phosphate) or porous for tissue ingrowth (hydroxyapatite-coated metals, alumina) may be used in the bioceramic composites [L.L. Hench et al.,1998]. Several types of bioactive glasses are developed during the last past fifty years. Bioactive glasses (BG) have been known for their bioactive properties and their ability to form a strong bond to the bone by the formation of hydroxyapatite surface layer [L.C. Gerhardt, and A. R. Boccaccini, 2010]. Bioactive glasses (BGs) such as “45S5 Bioactive glass having wt% composition (45SiO<sub>2</sub>-24.5CaO-24.5Na<sub>2</sub>O-6P<sub>2</sub>O<sub>5</sub>) [Hench, L. L. et. al. 1991] and “1393” having wt% composition (53SiO<sub>2</sub>-6Na<sub>2</sub>O-12K<sub>2</sub>O-5 MgO-20CaO-4P<sub>2</sub>O<sub>5</sub>) [Rahaman, M. N.; Day, D.

E.; Bal, B. S.; Fu, Q.; Jung, S. B.; Bonewald, L. F.; Tomsia, A. P.,2011] have been widely used for bone tissue engineering applications [A. Hoppe, B. Jokic, D. Janackovic, 2014].

[Hoppe et al. 2014] has developed cobalt oxide-releasing 1393 bioactive glass derivative scaffolds for bone tissue engineering applications as cobalt was known as angiogenesis agent. He has prepared a melt derived 1393 glass having wt% composition ( $53\text{SiO}_2\text{-}6\text{Na}_2\text{O}\text{-}12\text{K}_2\text{O}\text{-}5\text{MgO}\text{-}20\text{CaO}\text{-}4\text{P}_2\text{O}_5$ ) replaced CaO with CoO in the glass which was further used to produce a three-dimensional (3D) porous scaffolds by the foam replica technique. Structural properties of these bioactive glasses were studied by FTIR spectrometry. Thermal behavior, as well as scaffold macrostructure, compressive strength, acellular bioactivity and Co releases in simulated body fluid (SBF), were investigated. Replacement of CaO with CoO in 1393 bioactive glass was done from 1.0 to 2.5% by weight of cobalt oxide which has shown to act in a concentration-dependent manner as both network former as well as a modifier in the bioactive glass. The SBF investigation has done hoppe et.al [Hoppe et.al, 2014] for all glass scaffolds containing 1 to 2.5% cobalt oxide had shown the formation Ca-P layer incorporated with cobalt on the surface of scaffold samples. The maximum concentration of  $\text{Co}^{2+}$  ions around 12 ppm released in SBF after 21 days of the reaction was found to be within the therapeutic range of divalent cobalt. So, considering the impact of surface chemistry on cell attachment proliferation, the resulting formation of Ca-P layer is incorporated by  $\text{Co}^{2+}$  ions at the scaffolds-SBF interface would be very important for improving the understanding of mineralization behavior as well as cell response to bioactive scaffolds. The authors mentioned that these  $\text{Co}^{2+}$  releasing scaffolds could be used as hypoxia-mimicking novel biomaterials with a high degree of mechanical integrity, making them interesting candidates for bone tissue engineering applications [Hoppe et al., 2014].

Hench et al. have also investigated the in vitro bonding mechanism with synthetic material because of the chemical reactions taking place over the glass surface. These chemical reactions powerfully help the implants to bond with the bone tissues; hence one can replace the diseased or damaged part of the human bone [L.L. Hench, H.Oonishi, J. Wilson, Sugihara, E. Tsuji, M.Matsuura, S.Kin, T. Yamamoto and S.Mizokawa, 2000]. Most of the available work on bioactive material is concentrated on silica-based material. It is accepted that the essential requirements for an artificial biomaterial are to exhibit the formation of apatite or calcium phosphate layer on its surface in body environment. Unlike other bioactive materials, the rate of chemical reaction of bioactive glasses can easily be controlled by changing the chemical composition and heat treatment [H.A. ElBatal, M.A. Azooz, E.M.A. Khalil, A. Soltan Monem, Y.M. Hamdy, 2003]. Several new bioactive glass compositions have been developed, incorporating therapeutically active ions such as strontium [Fredholm YC, Karpukhina N, Law RV, Hill RG, 2010], zinc [Lusvardi G, Malavasi G, Menabue L, Menziani MC, 2002 and Aina V, Malavasi G, Pla AF, Munaron L, Morterra C, 2009], cobalt [Azevedo MM, Jell G, O'Donnell MD, Law RV, Hill RG, Stevens MM, 2010], fluoride [Brauer DS, Karpukhina N, O'Donnell MD, Law RV, Hill RG, 2010, Lusvardi G, Malavasi G, Cortada M, Menabue L, Menziani MC, Pedone A, et al 2008] and magnesia [Watts SJ, O'Donnell MD, Law RV, Hill RG, 2010]. Therefore bioactive silicate glasses are of interest for use as bone grafts. Inorganic species such as metal ions,  $\text{Cu}^{2+}$ ,  $\text{Sr}^{2+}$ , and  $\text{Co}^{2+}$  are being considered as a possible alternative to growth factors and genetic approaches in tissue engineering because of their easy processing, stability at high temperatures and tunable release kinetics [Kokubo T, Takadama H, Biomaterials 2006]. The  $\text{ZrO}_2$  ceramic is widely used as a substrate in hard tissue applications due to its excellent strength and fracture toughness [Hench LL, Wilson J,

editors, 1993]. It was discovered from the reaction product obtained after heating gems by the German chemist Martin Heinrich Klaproth in 1789 [Martin Heinrich Klaproth in 1789]. In the present investigation an attempt has been made to study the effect of zirconium dioxide substituting in silica-based 1393 bioactive glass and to find out its bioactivity and mechanical properties.

### 4.2 Experimental procedures

#### 4.2.1 Preparation of bioactive glasses

Fine-grained quartz was used as the source of  $\text{SiO}_2$ ,  $\text{Na}_2\text{O}$ , and  $\text{CaO}$  were introduced in the form of anhydrous sodium carbonate [ $\text{Na}_2\text{CO}_3$ ] and anhydrous calcium carbonate [ $\text{CaCO}_3$ ] respectively.  $\text{P}_2\text{O}_5$  was added in the form of ammonium dihydrogen orthophosphate [ $\text{NH}_4\text{H}_2\text{PO}_4$ ].  $\text{K}_2\text{O}$  and  $\text{MgO}$  have introduced in the form of potassium carbonate [ $\text{K}_2\text{CO}_3$ ] and magnesium carbonate [ $\text{MgCO}_3$ ] respectively [A. Hoppe, B. Jokic, D. Janackovic, 2014]. The  $\text{ZrO}_2$  is available as it is and was used to replace  $\text{SiO}_2$  for preparation of substituted bioactive glasses. All the batch materials were of analytical grade chemicals and were used without further purification. The compositions of bioactive glasses are given in the Table-4.1. The weighed batches were correctly mixed with the help of mortar and pestle. Before mixing the mortar and pestle were cleaned thoroughly and allowed to dry properly. After thorough mixing of batch materials, they were put in alumina crucibles and placed in an electric furnace. The furnace temperature was set to  $1350^\circ\text{C}$ , and after reaching  $1350^\circ\text{C}$  the steady-state was maintained for more than 3 hours. After melting the prepared bioactive glasses were poured onto aluminum molds and were directly transferred to a regulated muffle furnace at the temperature of  $550^\circ\text{C}$  for annealing. The muffle furnace was left to cool to room temperature after 2 hour. Annealing is done to remove the internal stress after the

glasses are formed. Those glasses which are not annealed they are liable to crack upon sudden change of temperature i.e. any kind of thermal shock or if they get any kind of mechanical shock. The glass is heated until the temperature reaches a stress-free point that is at the annealing temperature (also called annealing point) at a viscosity ( $\eta$ ) of  $10^{13.4}$  poise.

Table 4.1- Composition of 1393 bioactive glass (wt %)

	SiO <sub>2</sub>	Na <sub>2</sub> O	CaO	P <sub>2</sub> O <sub>5</sub>	ZrO <sub>2</sub>	K <sub>2</sub> O	MgO
<b>Zr-0</b>	53.00	6.00	20.00	4.00	0.00	12.00	5.00
<b>Zr-1</b>	52.50	6.00	20.00	4.00	0.50	12.00	5.00
<b>Zr-2</b>	52.00	6.00	20.00	4.00	1.00	12.00	5.00
<b>Zr-3</b>	51.50	6.00	20.00	4.00	1.50	12.00	5.00
<b>Zr-4</b>	51.00	6.00	20.00	4.00	2.00	12.00	5.00

#### 4.2.2 Preparation of simulated body fluid (SBF)

Kokubo and his teams developed a cellular simulated body fluid that has inorganic ion concentrations similar to those of human extracellular fluid, in order to reproduce the formation of apatite on bioactive materials in vitro [Kokubo T, Takadama H, Biomaterials 2006]. This fluid can be used for not only evaluation of bioactivity of artificial materials in vitro, but also the coating of apatite on various materials under biomimetic conditions [Kokubo T, Takadama H, Biomaterials 2006]. The simulated body fluid is often abbreviated as SBF or Kokubo solution. The ion concentrations of SBF are given in Table 4.2.

Table 4.2- Ion concentration (mM/litre) of SBF and human blood plasma

Ion	Na <sup>+</sup>	K <sup>+</sup>	Mg <sup>2+</sup>	Ca <sup>2+</sup>	HCO <sub>3</sub> <sup>-</sup>	HPO <sub>4</sub> <sup>-</sup>	SO <sub>4</sub> <sup>2-</sup>	Cl <sup>-</sup>
Simulated body fluid	142.0	5.0	1.5	2.5	4.2	1.0	0.5	147.8
Human blood plasma	140.0	5.0	1.5	2.5	27.0	1.0	0.5	103.0

### 4.2.3 X-ray diffraction analysis

To identify the crystalline phase present in the 1393 bioactive glasses and SBF treated glass samples, the samples were ground to 75 $\mu$ m and the fine powders were subjected to X-ray diffraction analysis (XRD) using RIGAKU-Miniflex II diffractometer adopted Cu-K $\alpha$  radiation ( $\lambda = 1.5405 \text{ \AA}$ ) with a tube voltage of 40 kV and current of 35 mA in a  $2\theta$  range between 20° and 80°. During measurement, the step size and speed were set to 0.02° and 1° per min respectively. The JCPDS-International Centre for diffraction Data Cards were used as a reference.

### 4.2.4 In vitro bioactivity of 1393 bioactive glass

The bioactivities of the prepared bioactive glass samples were examined. The experiment was performed by immersing 0.2 gram of each bioactive glass samples in 20 ml of SBF solution contained in a small plastic container (50 ml) and incubated at 37.5 °C in a static condition for time periods of 0, 2, 8 and 20 days. After soaking, the 1393 bioactive glass for different time period samples were filtered, rinsed with double distilled water and dried in an electric air oven at 110 °C for 3 h. The formation of hydroxyl carbonate apatite layer (HCA) on the surface of the 1393 bioactive glass samples were determined using FTIR and SEM techniques.

### 4.2.5 Structural analysis of bioactive glasses

The functional groups of 1393 bioactive glasses were investigated at room temperature in the wave number range of 4000–400  $\text{cm}^{-1}$  using a Fourier transform infrared (FTIR) spectrometer (VARIAN scimitar 1000, USA). The fine 1393 bioactive glass powder samples and KBr were mixed in the ratio of 1:100 respectively and these mixtures were subjected to an evocable die at the load of 12 MPa to produce clear



homogeneous discs. The discs were immediately subjected to IR spectrometer to measure the absorption spectra in order to avoid a damp attack. The sample (two grams) was immersed in 20 ml of SBF solution in a plastic container at 37.5°C with pH 7.4 in an incubator at the static condition for the time period of 0, 2, 8, and 20 days. After soaking, the bioactive glass samples were filtered and dried in an oven at 110°C for 3 hours, before FTIR analysis is done.

### 4.2.6 pH measurements

The glass powders (0.2 grams) were soaked in 20 ml of SBF solution at 37.5°C for different time periods like (0, 2, 8, and 20 days) and the pH was measured using Universal Bio Microprocessor pH meter. The pH meter was calibrated each time with standard buffer solutions of pH 4.00 and 7.00 at room temperature and pH values have been corded during different time periods at a fixed time interval.

### 4.2.7 Density and mechanical properties measurements

The melts were cast in a rectangular shaped mold, and the resultant bioactive glass samples were ground and polished for required dimension using grinding machine and then samples were subjected to three-point bending test. The test was performed at room temperature using Instron Universal Testing Machine (AGS 10kND, SHIMADZU) of the cross-head speed of 0.5 mm/min and the full-scale load of 2500 kg. Flexural strength was determined using the formula -1.

$$[\sigma_f = (3P_f L)/(2bh^2)] \text{ - - - - - (1)}$$

Where  $P_f$  is the load at which specimen being fractured,  $L$  is the length over which the load is applied,  $b$  is the width and  $h$  is height of sample.

(10mm x 10mm x 10 mm) size of polished 1393 bioactive glass and zirconium dioxide substituted bioactive glasses were prepared according to ASTM standard: C730-98. The indentations have been made for loads ranging between 30 mN and 2000 mN, applied at a velocity of 1 mm/s and allowed to equilibrate for 16 second before measurement. Micro hardness, H (GPa) of 1 mm/s was calculated using the formula (2).

$$H = 1.854 (P/d^2) \quad \text{--- (2)}$$

Where P (N) is the applied load on sample and d (m) is the diagonal of the impression

Compressive strength of the base glass and ZrO<sub>2</sub> substituted bioactive glass is (2 x 2 x 1 cm<sup>3</sup> size) were subjected to compression test according to ASTM D3171. The test was performed using Instron Universal Testing Machine at room temperature (cross speed of 0.05 cm/min and full scale of 5000 kgf).

The densities of base 1393 bioactive glass and zirconium dioxide substituted 1393 bioactive glasses were measured by Archimedes principle with water as the immersing fluid. The measurements were performed at room temperature. All the weight measurements have been made using a digital balance [Sartorius, Model: BP221S, USA] having an accuracy of ± 0.0001 g. Density (ρ) of sample was obtained by using the relation as given below in equation (3).

$$\text{Density} = [Ma / (Ma - Mi)] \times 0.988 \quad \text{--- (3)}$$

Where, Ma (weight of sample in air) and Mi (weight of sample in water)

### 4.2.8 SEM of 1393 bioactive glasses

The surface morphology of samples was analyzed by scanning electron microscope (SEM) after SBF treatment (Inspect S50, FEI). The bioactive glass powders (2g) were pressed (load of 10 MPa) into pellet forms in a hand pelletizer machine using an evocable die to produce discs of 10 mm in diameter. The Poly (vinyl alcohol) (PVA) was used as a binder for making pellets. The pellets were immersed in SBF (20 ml) for 8 days at 37.5°C. They were coated with gold (Au) by sputter coating instrument before their examination with SEM.

## 4.3 Results and discussion

### 4.3.1 X-ray diffraction (XRD) patterns of 1393 bioactive glasses

The X-ray diffraction (X-RD) patterns for 1393 bioactive glass and zirconium dioxide substituted 1393 bioactive glasses are shown in **Figure:-4.1**. The observed results indicate that the glasses have amorphous structure and there is no indication for the presence of crystalline phases. It was observed that as the concentration of zirconium dioxide was increased in the composition the broad hump at  $2\theta$  between  $25^\circ$  to  $35^\circ$  become more intense.

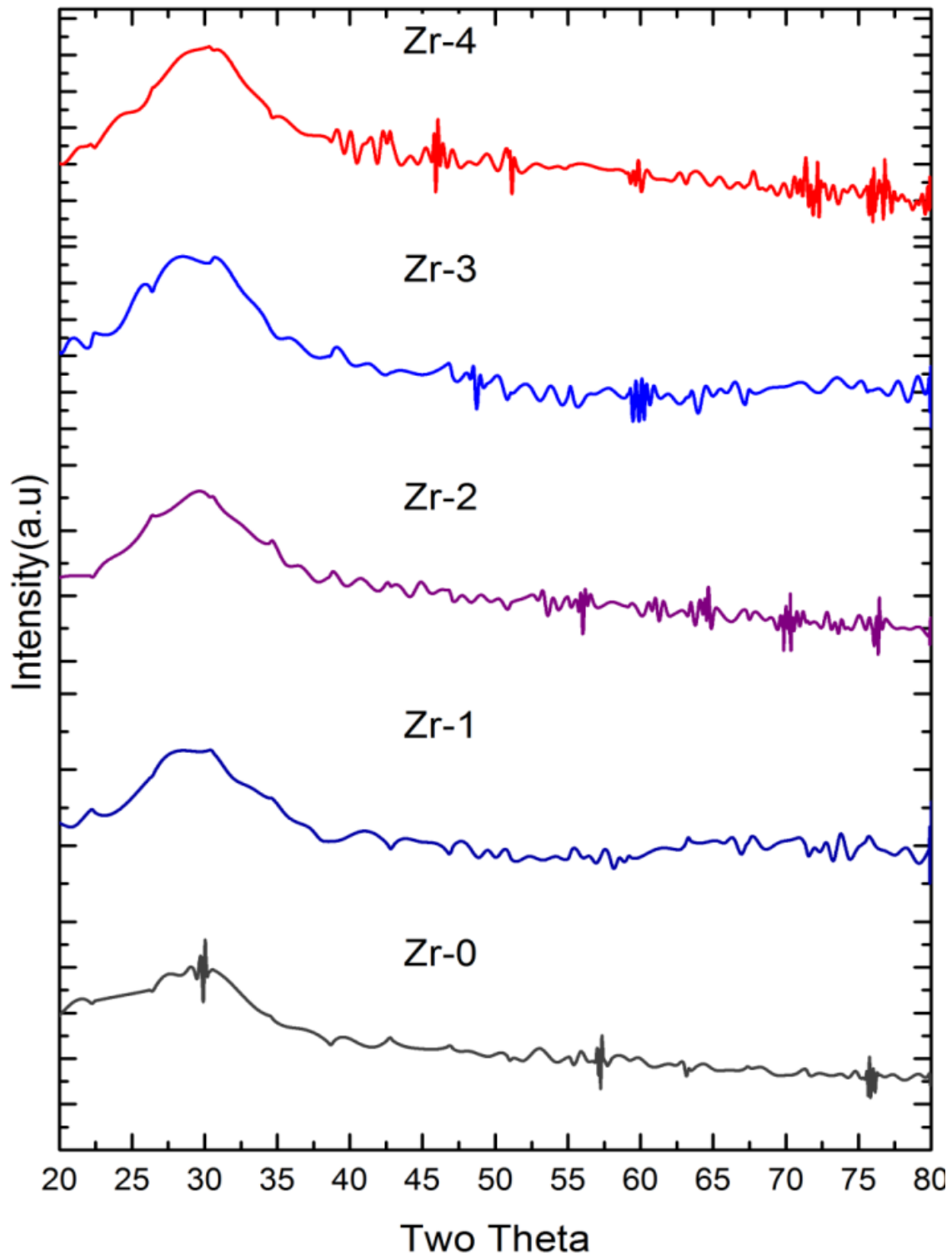


Figure 4.1- XRD of the bioactive glasses

### 4.3.2 FTIR reflection spectra of 1393 bioactive glasses

Figure:-4.2 shows the FTIR Reflection spectra of the 1393 and zirconium dioxide substituted bioactive glass before SBF treatment. All the bioactive glass samples are showing similar trend behavior, FTIR Reflection spectra bands of all the glasses confirm the main characteristic of silicate network and this may be due to the presence of SiO<sub>2</sub> as a major constituent. The bioactive glass (Zr-1) shows the peaks at 439, 927, 1037, 1494 and 2800-3800 cm<sup>-1</sup> respectively. The resultant IR spectra at 439 cm<sup>-1</sup> associated with Si–O–Si symmetric of bending mode. The band at 927 cm<sup>-1</sup> corresponds with Si–O–Si symmetric stretch of non-bridging oxygen atoms between tetrahedral. It was observed that the intensity of the band recreated as the zirconium dioxide substituted in the 1393 bioactive glasses; therefore, the zirconium dioxide increases the non-bridging oxygen in the network. The major band at about 1037 cm<sup>-1</sup> can be attributed to Si-O-Si stretching. The small band at 1494 cm<sup>-1</sup> attributed to C–O vibration mode. It was observed that the intensity of the IR peak had been increased as the concentration of zirconium dioxide increased. This is due to the breaking of the Si–O–Si bond, which holds the glass structure together. The small, broadband centered at about 2800-3800 cm<sup>-1</sup> can be assigned to the hydroxyl group (–OH) which may be the presence of adsorbed water molecules. This represents the infrared frequencies and related functional, structural groups in the bioactive glass [Nayak, J. P.; S. Kumar; J. Bera, 2010]. The bioactive glasses substituted with zirconium dioxide are not showing noticeable changes in the IR spectral bands.

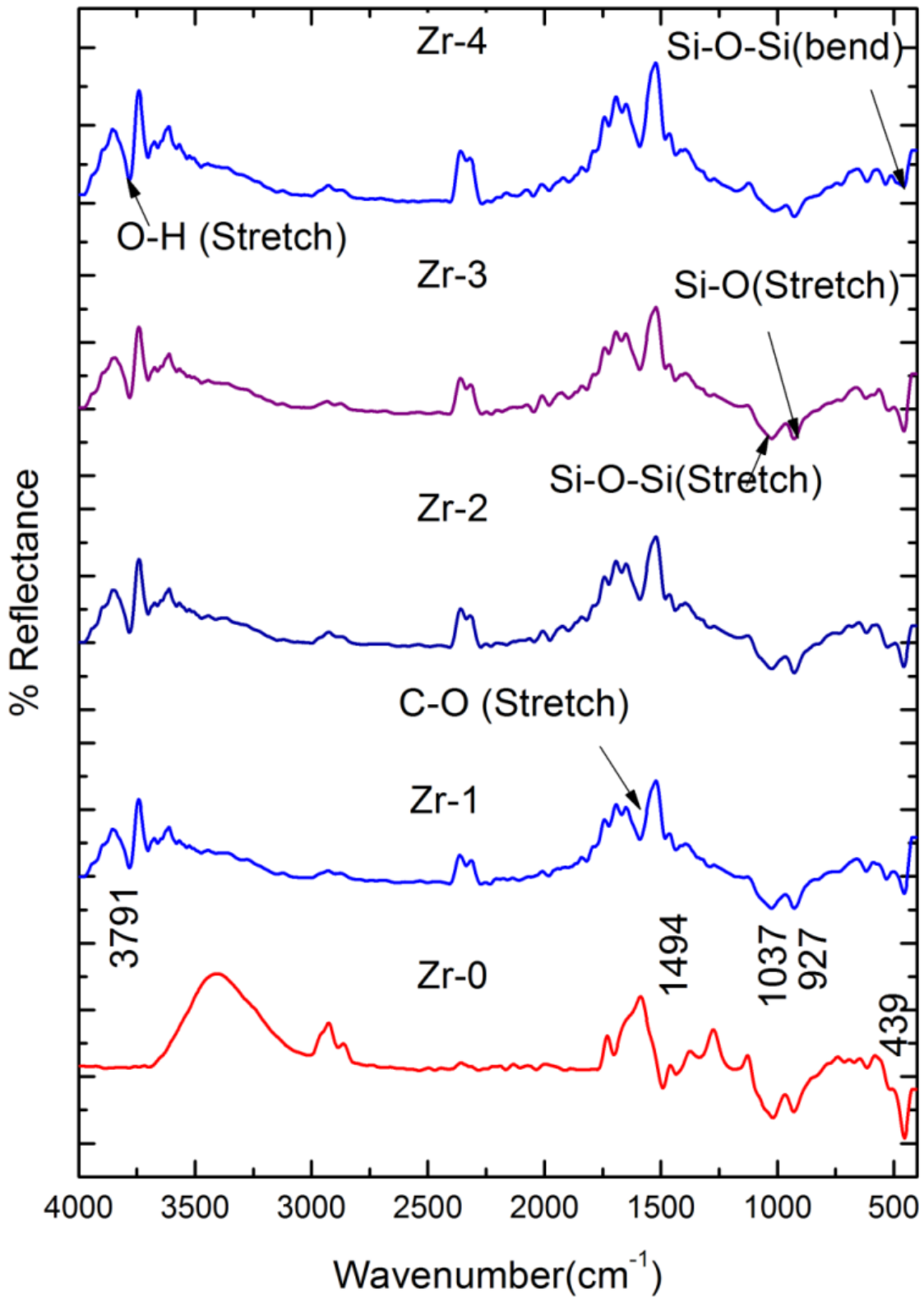


Figure 4.2- FTIR of the bioactive glasses

### 4.3.3 pH behaviors base and doped bioactive glasses in SBF

Figure.4.3 shows variation in pH values of bioactive glass after soaking into simulated body fluid (SBF) for 0, 2, 8, and 20 days. It was observed that up to 8 days, all bioactive glasses are showing an increase in pH values almost linearly from pH value 7.4. The Zr-2 bioactive glass is showing maximum pH value on 8th day i.e., 9.02. Due to the addition of zirconium dioxide, there are variations in the pH values for different samples. The Zr-2 bioactive glass is showing maximum pH at the end of 20th day. The Zr-2, which consists of 1 wt% of zirconium dioxide, is showing maximum pH value. It was found that in all cases the pH value was decreasing after 8 days and attended a constant value up to 20th days. The increase in pH values of bioactive glass in SBF solution is due to release of  $\text{Ca}^{2+}$  and  $\text{Na}^{2+}$  ions from the sample surface [Nayak, J. P.; S. Kumar; J. Bera 2010]. The sample number Zr-2 with higher zirconium dioxide content was found to show maximum pH value may be due to the high rate of dissolution as compared to base bioactive glass sample Zr-0. The incorporation of zirconium dioxide into 1393 bioactive glass resulted in an increase in the pH of SBF. Their high degradation rate leads to higher pH value, and this agrees to the condition of formation of hydroxylapatite like layer on the surface of the samples with more crystalline.

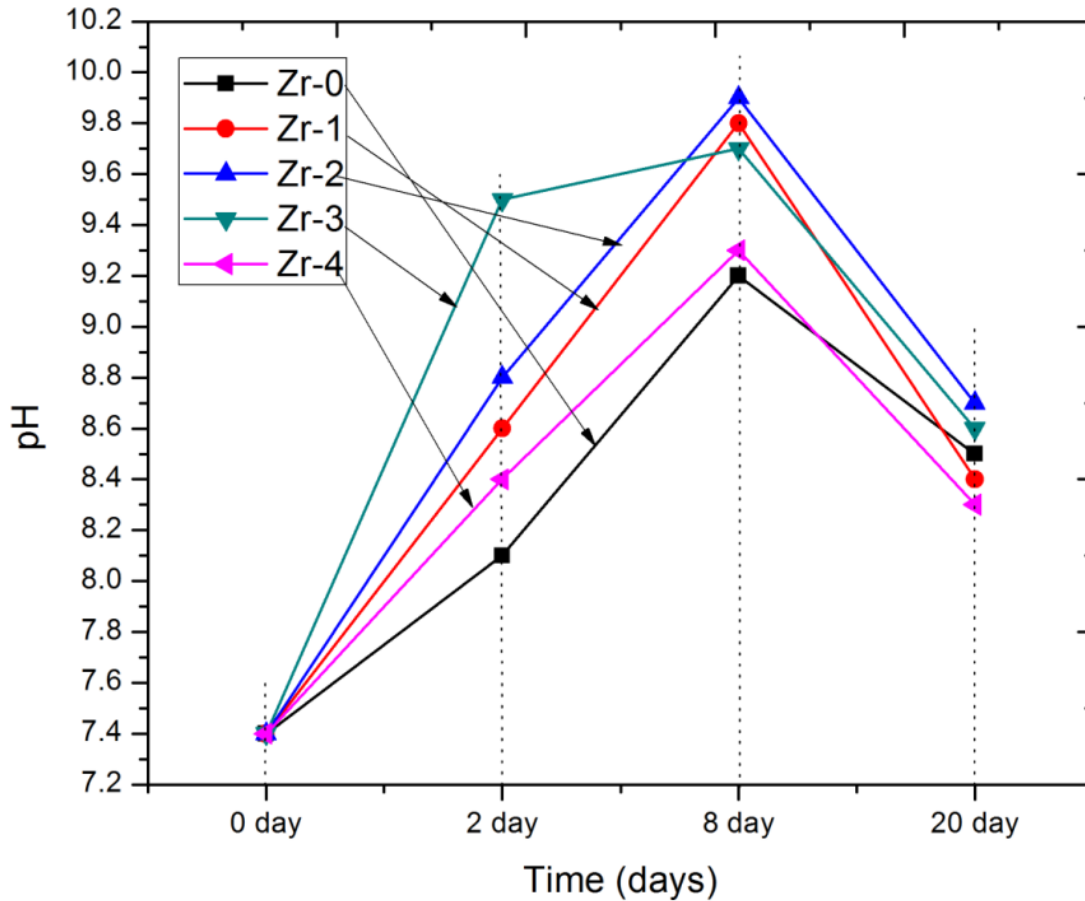


Figure 4.3- pH behavior of the SBF after immersion of the bioactive glasses

#### 4.3.4 In vitro bioactivity of 1393 and doped bioactive glasses by FTIR reflectance spectrometry

Figure: - 4.4, 4.5, 4.6, & 4.7 show the FTIR Reflection spectra bands of the bioactive glass before and after immersing in SBF for different period of times days 0, 2, 8 and 20 [L.L. Hench et al., 1998 and C.Y. Kim, A.E. Clark, L.L. Hench, 1989]. Hench et al., 1998 [L.L. Hench et al., 1998] and Kim et al., 1989 [C.Y. Kim, A.E. Clark, L.L. Hench, 1989] confirmed that effect in the IR spectra bands after immersing in SBF for prolonged-time period and the stages of apatite formation on the surface of the samples after soaking in SBF.



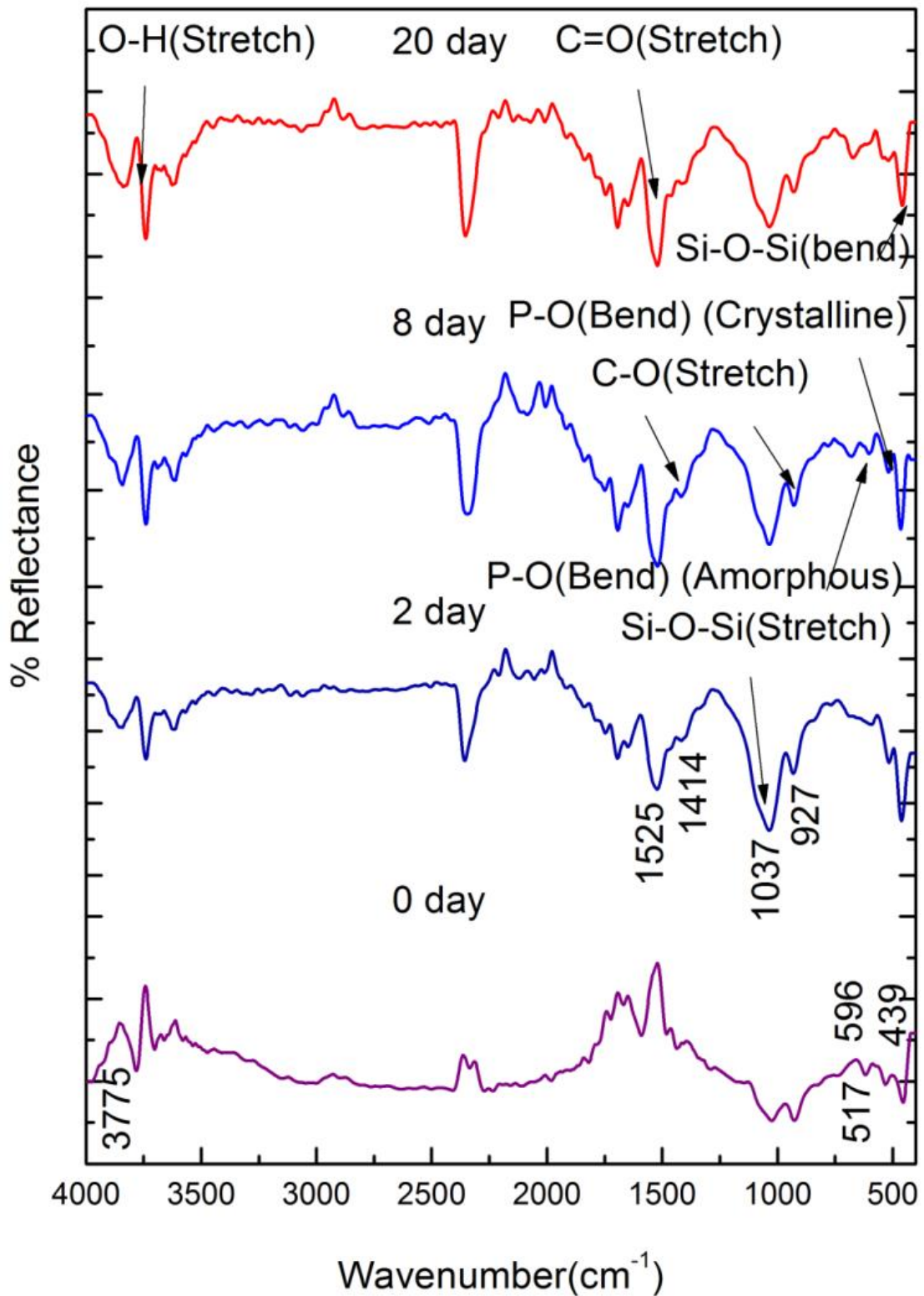


Figure 4.4- FTIR of the bioactive glass (Zr-1) before and after immersion in SBF for (0, 2, 8 and 20) days

**Figure: - 4.4** shows the IR spectra bands of Zr-1 sample before and after treated with SBF. The new groups have appeared after 2-day immersion in SBF when

compared to before immersion at 517, and 596  $\text{cm}^{-1}$  corresponds to P–O bending (crystalline) and P–O bending (amorphous) bending respectively. Presence of C–O stretching at 927  $\text{cm}^{-1}$  band shows the crystalline nature indicates the formation of hydroxyl carbonate apatite (HCA) layer. The bands at about 1414 and 1525  $\text{cm}^{-1}$  are associated with C–O (Stretch) and C=O (Stretch) stretching mode and the broadband at about 2800–3800  $\text{cm}^{-1}$  can be assigned to (hydroxyl) O–H groups on the surface. The prolonged period of the samples in SBF shows the same behavior with a small decrease in the intensities of the bands, which are resulted in favor of the development of hydroxyl carbonated apatite (HCA) layer.

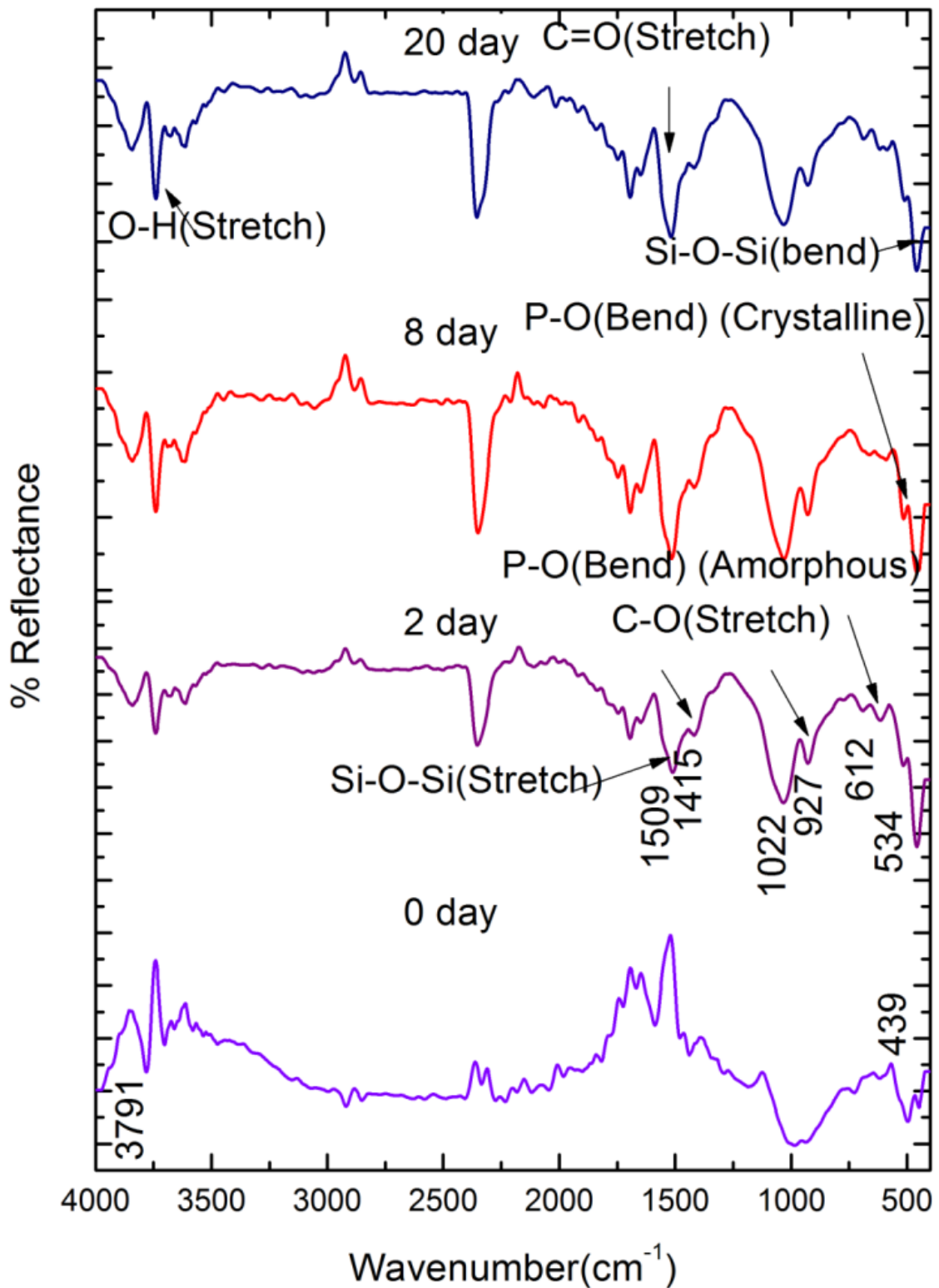


Figure 4.5- FTIR of the bioactive glass (Zr-2) before and after immersion in SBF for (0, 2, 8 and 20) days

**Figure: - 4.5** shows the IR spectra bands of Zr-2 sample before and after treated with SBF. The new bands have appeared after 2-day immersion in SBF when compared

to before immersion at 534, and 612  $\text{cm}^{-1}$  corresponds to P–O bending (crystalline) and P–O bending (amorphous) bending respectively. Presence of C–O stretching at 927  $\text{cm}^{-1}$  band shows the crystalline nature indicates the formation of hydroxyl carbonate apatite (HCA) layer. The bands at about 1415 and 1509  $\text{cm}^{-1}$  are associated with C–O (Stretch) and C=O (Stretch) stretching mode and the broadband at approximately 2800–3800  $\text{cm}^{-1}$  can be assigned to (hydroxyl) O–H groups on the surface. The protracted period of the samples in SBF shows the same trend with a small decrease in the intensities of the bands, which are resulted in favor of the development of hydroxyl carbonated apatite (HCA) layer.

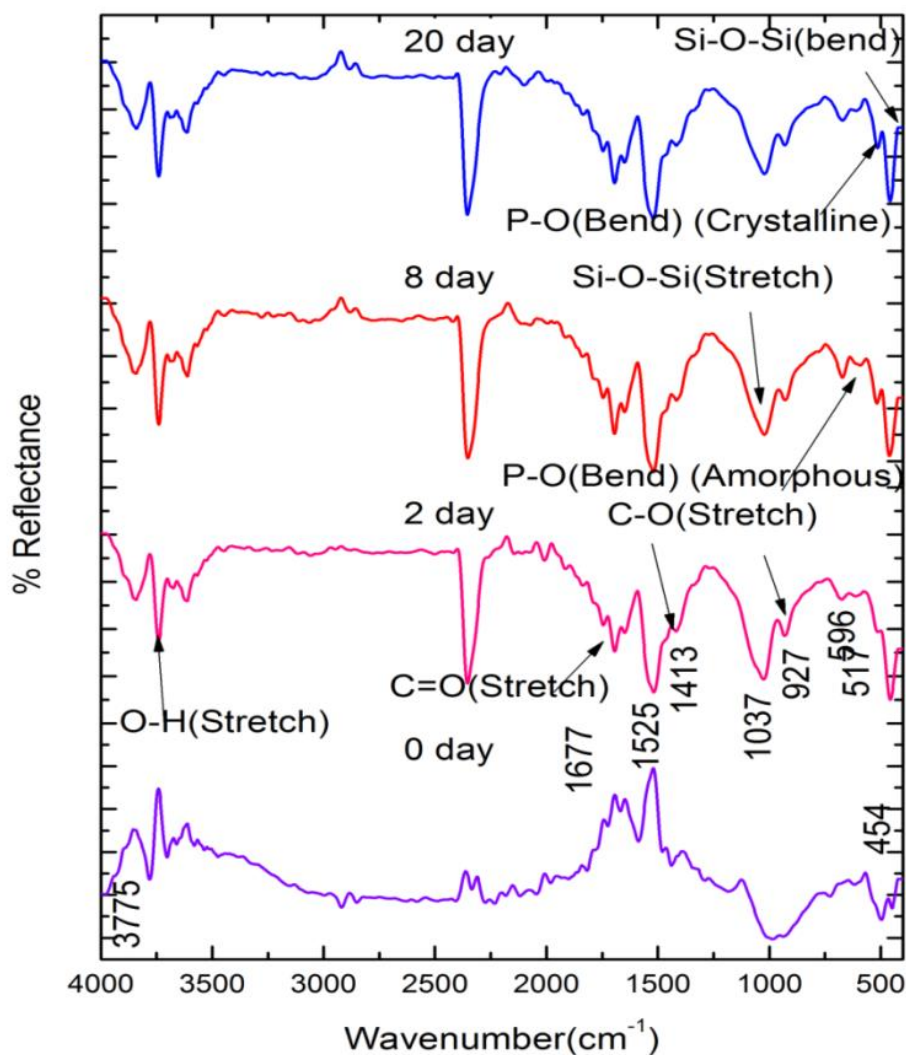


Figure 4.6- FTIR of the bioactive glass (Zr-3) before and after SBF for (0, 2, 8 and 20) days

**Figure: - 4.6** shows the IR spectra bands of Zr-3 sample before and after treated with SBF. The new bands have appeared after 2-day immersion in SBF when compared to before immersion at 517 and at 596  $\text{cm}^{-1}$  are corresponds to P–O bending (crystalline) and P–O bending (amorphous) bending respectively. Presence of C-O stretching at 927  $\text{cm}^{-1}$  bands show the crystalline nature indicates the development of hydroxyl carbonate apatite (HCA) layer. The bands at about 1413 and 1525  $\text{cm}^{-1}$  are associated with C-O (Stretch) and C=O (Stretch) stretching mode and the broadband at approximately 2800-3800  $\text{cm}^{-1}$  can be assigned to (hydroxyl) O-H groups on the fine surface. The protracted period of the samples in SBF shows the same behavior with a small decrease in the intensities of the bands, which are resulted in favor of the development of hydroxyl carbonated apatite (HCA) layer.

**Figure: - 4.7** shows the IR spectra bands of Zr-4 sample before and after treated with SBF. The new bands have appeared after 1-day immersion in SBF when compared to before immersion at 518, and 659  $\text{cm}^{-1}$  corresponds to P–O bending (crystalline) and P–O bending (amorphous) bending respectively. Presence of C-O stretching at 926  $\text{cm}^{-1}$  bands show the crystalline nature indicates the development of hydroxyl carbonate apatite (HCA) layer. The bands at about 1541 and 1697  $\text{cm}^{-1}$  are associated with C-O (Stretch) and C=O (Stretch) stretching mode and the broadband at approximately 2800-3800  $\text{cm}^{-1}$  can be assigned to (hydroxyl) O-H groups on the surface. The prolonged period of the samples in SBF shows the same behavior with a small decrease in the intensities of the bands, which are resulted in favor of the development of hydroxyl carbonated apatite (HCA) layer.

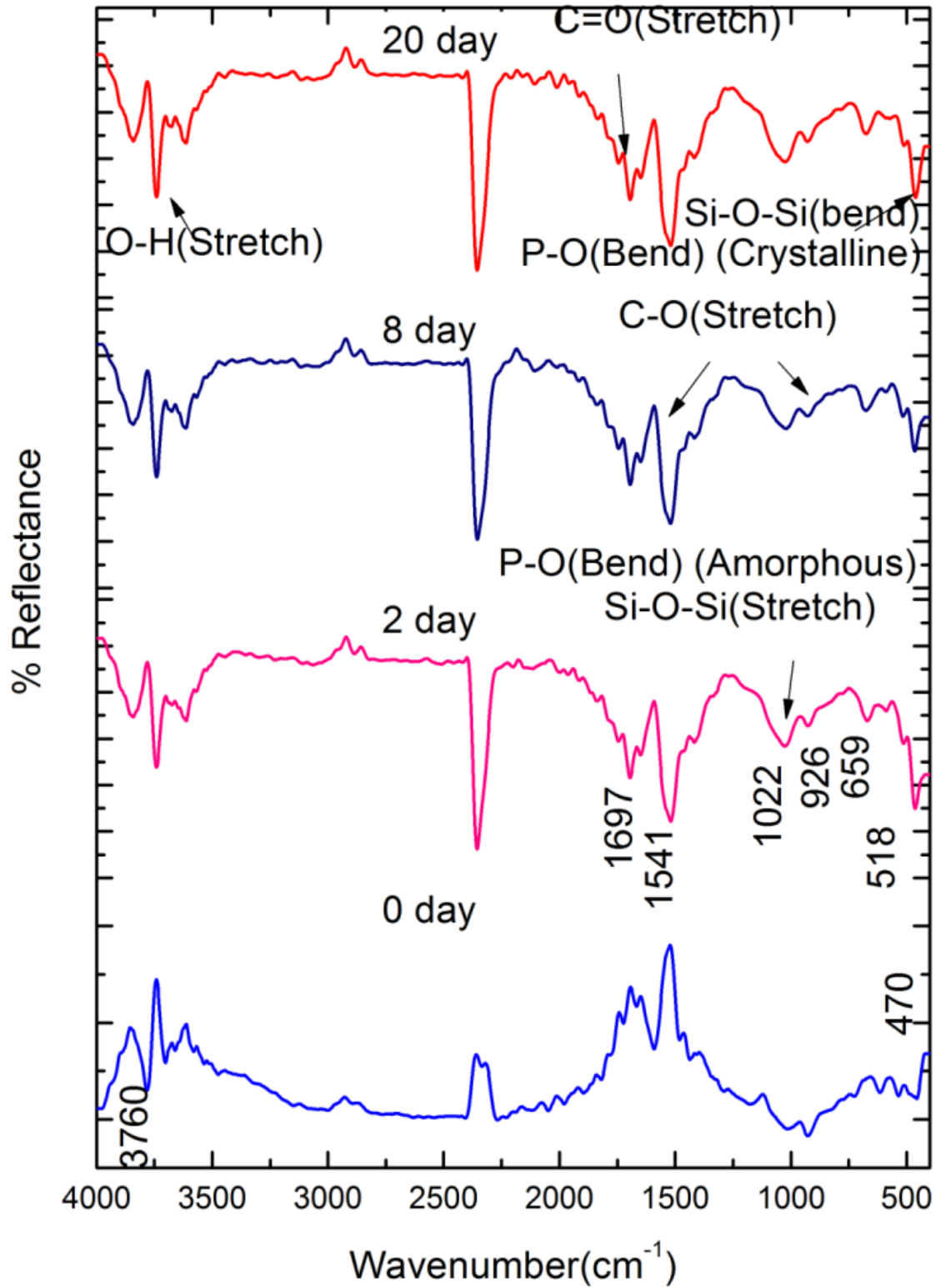


Figure 4.7- FTIR of the bioactive glass (Zr-4) before and after immersion in SBF for (0, 2, 8 and 20) days

#### 4.3.5 Mechanical behavior of Zr-0, Zr-1 Zr-2, Zr-3 and Zr-4 bioactive glasses

**Figure: - 4.8** show the density of zirconium dioxide substituted 1393 bioactive glass. It is observed that the densities of the samples were increased with increasing zirconium dioxide content from 2.78 to 2.96 gm/cm<sup>3</sup>, which may be due to partial replacement of SiO<sub>2</sub> with ZrO<sub>2</sub>. This is attributed due to the replacement of a light element (density of SiO<sub>2</sub> -2.64) with a heavier one (ZrO<sub>2</sub> 5.68). A similar trend of results also found in the compressive strength (Zr-0, Zr-1 Zr-2, Zr-3 and Zr-4 - 61.82, 73.72, 76.92, 77.98 and 81.13 MPa respectively) shown in **Figure: - 4.8**.

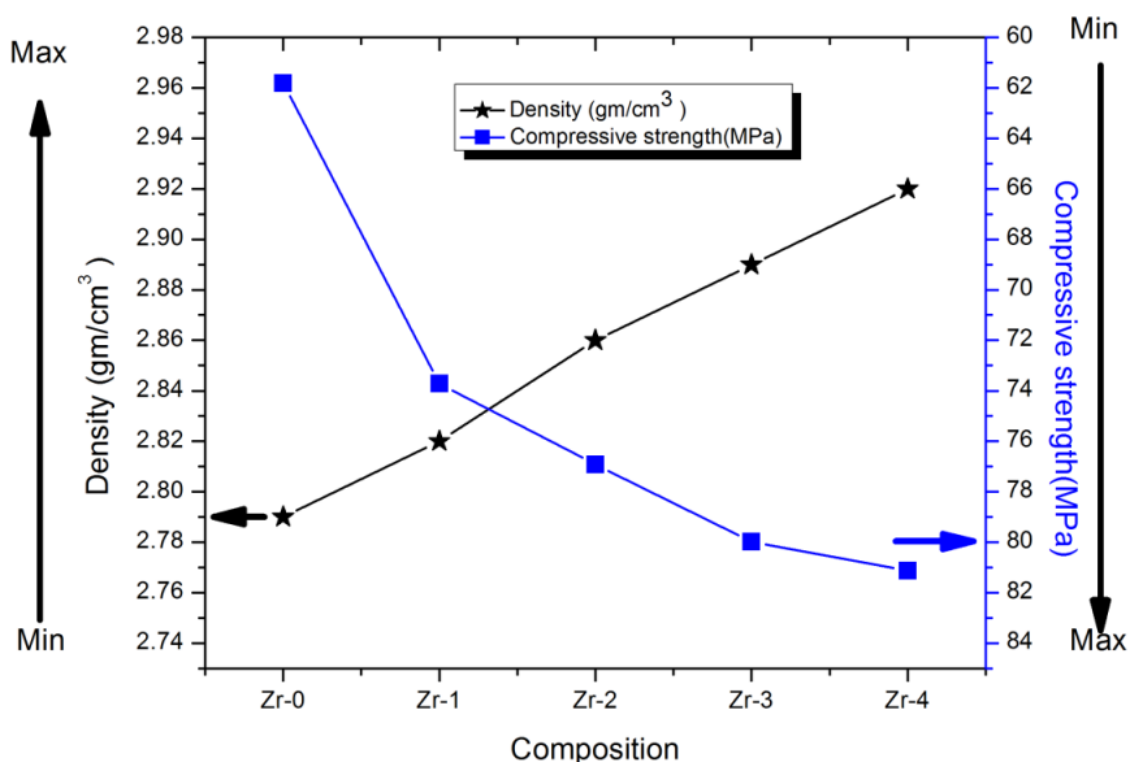


Figure 4.8- Density and compressive strength of the 1393 bioactive glass samples

**Figure: -4.9** shows the results of the flexural strength and Microhardness of Zr-0, Zr-1 Zr-2, Zr-3, and Zr-4 samples. The results demonstrate an increasing tendency in flexural strength and Microhardness as the percentage of zirconium dioxide increase (44.48, 57.25, 59.42, 61.52 and 68.58 Microhardness 5.85, 5.88, 5.91, 5.97 and 5.99 respectively). This increase may be due to the Zr<sup>4+</sup> may act as network intermediate,



thus more the compactness of glass structure. Vyas et al., [Vikash Kumar Vyas, Arepalli Sampath Kumar, S. P. Singh, and Ram Pyare, 2016] in an earlier investigation had also shown that the addition of cobalt oxide up to 2.0 wt% in 45S5 glass & glass-ceramic has resulted in an increase in density and compressive strength, flexural strength and Microhardness [Vikash Kumar Vyas , Arepalli Sampath Kumar , S. P. Singh and Ram Pyare 2016]. Vyas et al. [Vikash Kumar Vyas, Arepalli Sampath Kumar, S. P. Singh, Akher Ali1, Sunil Prasad, Md. Ershad Pradeep Srivastava, Sarada Prasanna Mallick and Ram Pyare 2016] investigated assessment of nickel oxide substituted bioactive glass-ceramic on in vitro bioactivity and mechanical properties. They have prepared a melt derived 45S5 glass having wt% composition (45SiO<sub>2</sub>-24.5Na<sub>2</sub>O-24.5CaO-6P<sub>2</sub>O<sub>5</sub> wt %) substituted with CoO for SiO<sub>2</sub> in the glass and found that density and compressive strength, flexural strength and micro hardness have increased with increasing CoO content [Hanan H. Beherei, Khaled R. Mohamed and Gehan T. El-Bassyouni. (2009)].

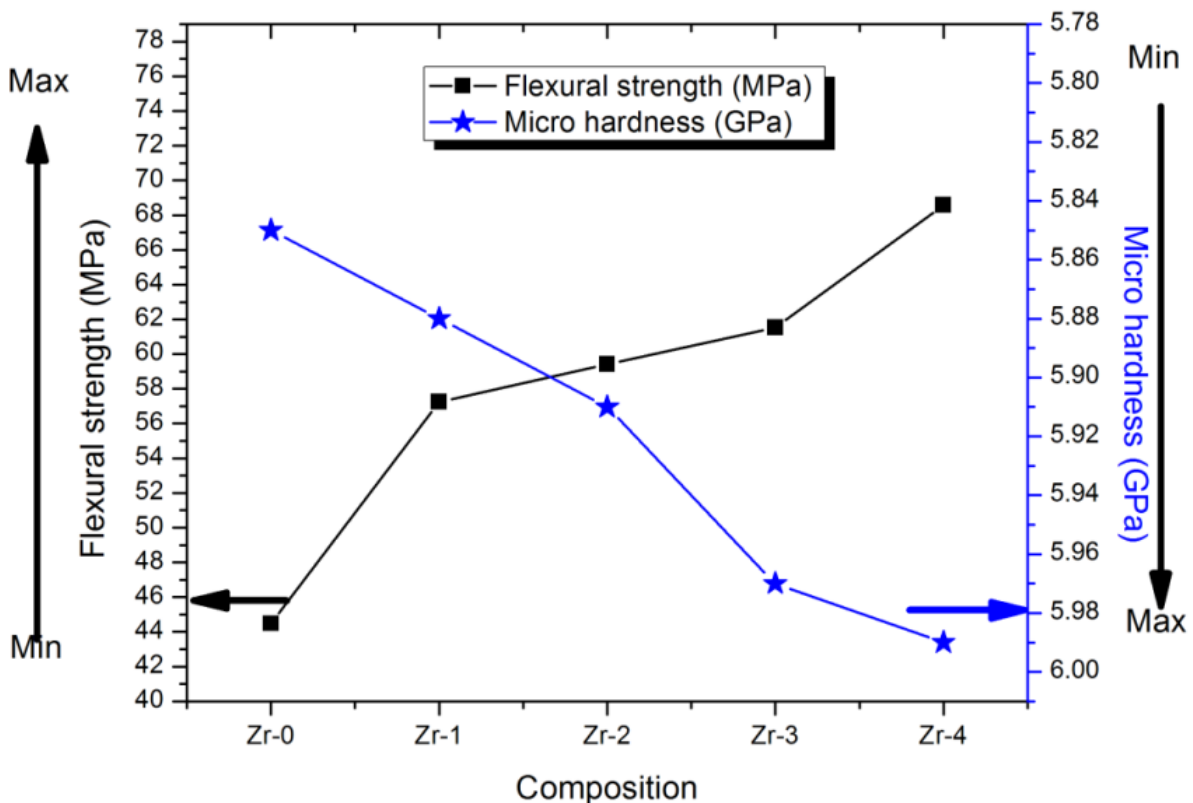


Figure 4.9- Flexural strength and micro hardness of the 1393 bioactive glasses



### 4.3.6 Scanning electron microscopy (SEM)

The SEM micrographs of 1393 glass and zirconium dioxide substituted glass samples before immersing in SBF solution are shown in **Figure:- 4.10**. This Figure shows different rod types of structure and asymmetrical grain of 1393 bioactive glass samples and is quite similar to the results found by Hanan et al. 2009 [32]. **Figure: - 4.11** represent the SEM micrographs of Zr-0 and (Zr-1, Zr-2, Zr-3, Zr-4) bioactive glass of after immersed in SBF solution for 8 days. It is observed from the Figure: -11 that Zr-0 and ( Zr-1,Zr-2,Zr-3,Zr-4) glass samples which were immersed in SBF solution for 8 days were enclosed with an asymmetrical shape and grounded HA particles have been grown into more than a few agglomerates consisting of spine shaped HA layer. These micrographs show the formation of HA on the surface of the Zr-0 and (Zr-1, Zr-2, Zr-3, Zr-4) glass samples after immersing in SBF solution for 8 days.

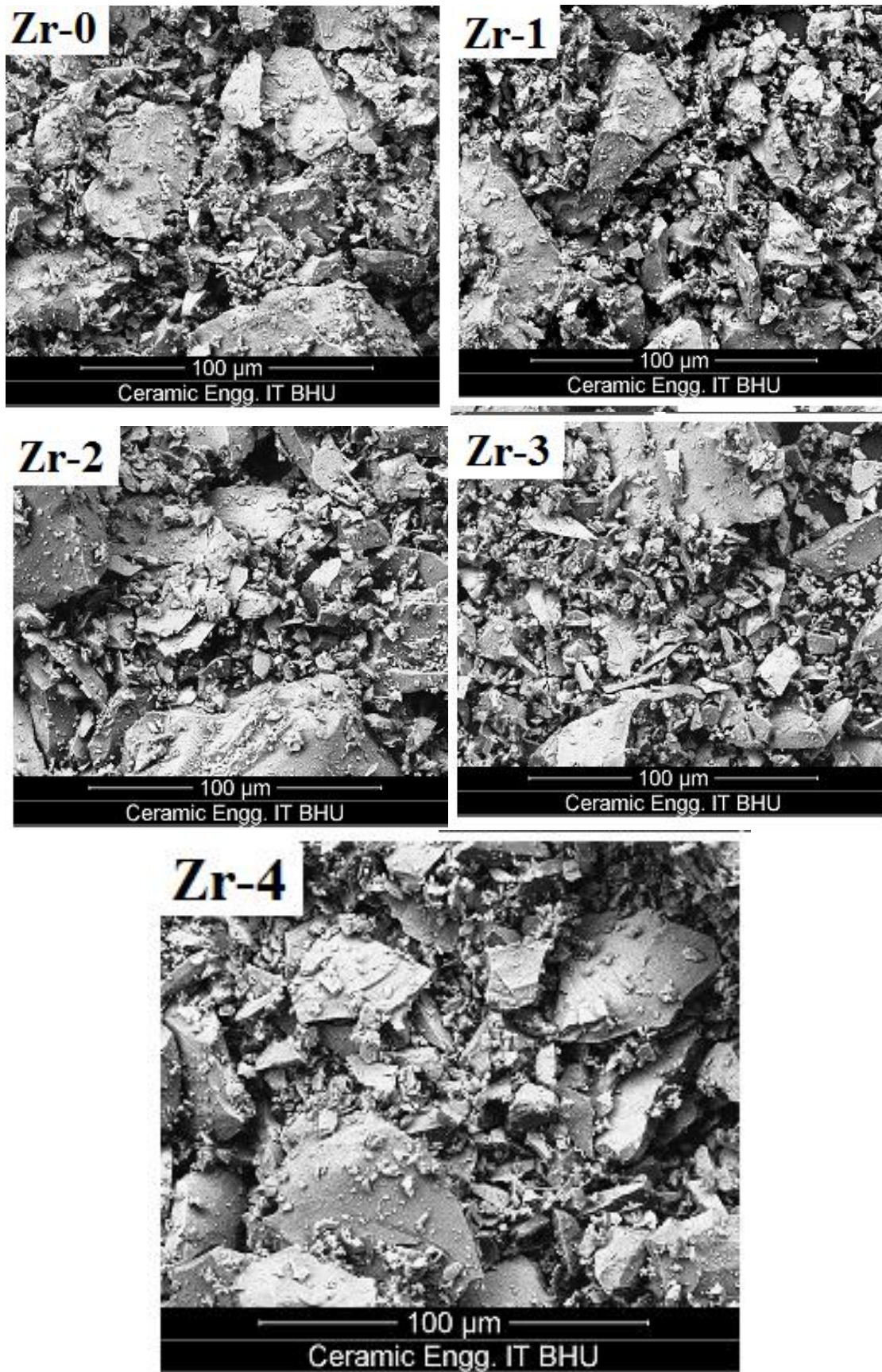


Figure 4.10- Scanning electron microscope (SEM) of bioactive glasses before immersion in SBF



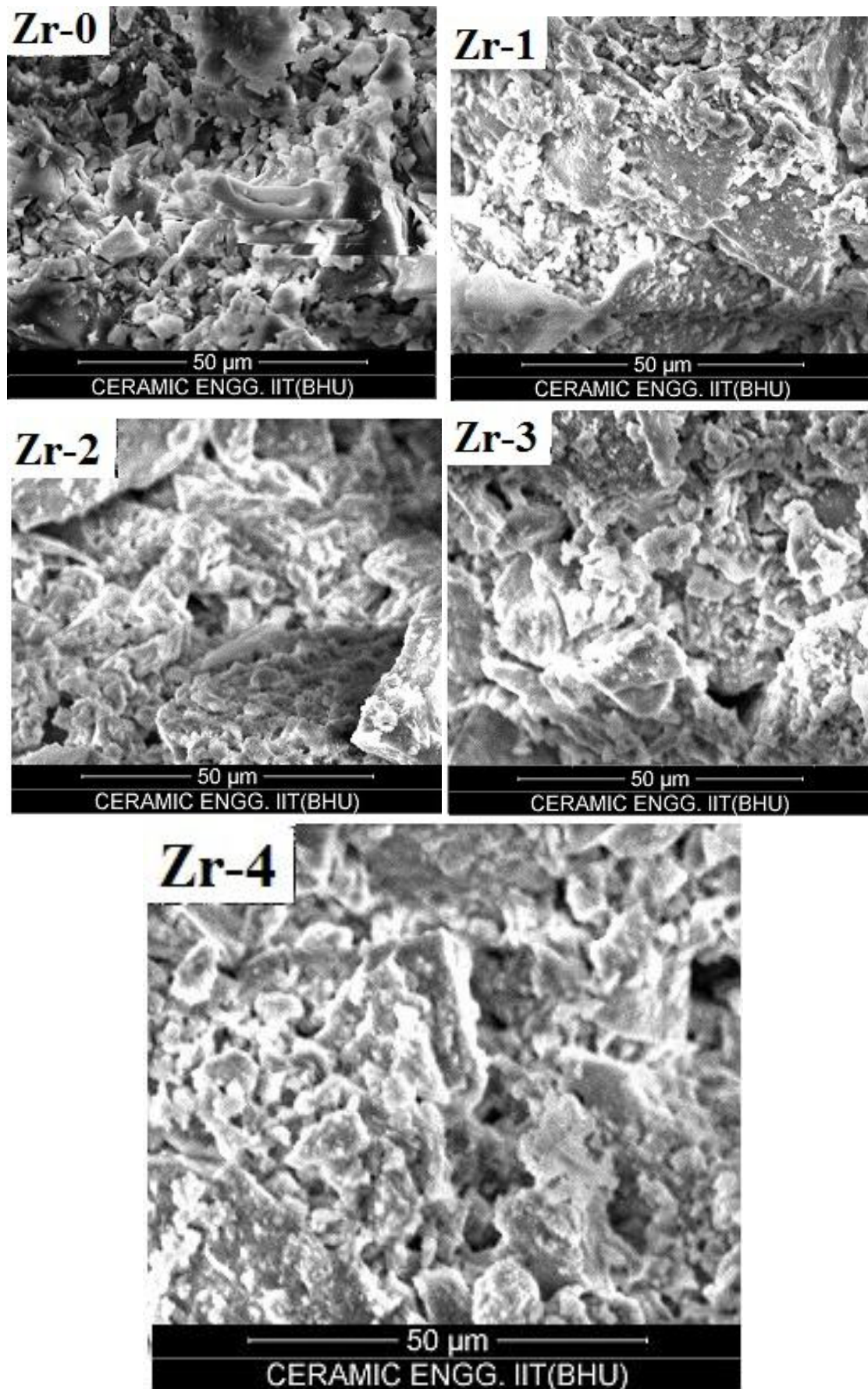


Figure 4.11- Scanning electron microscope (SEM) of bioactive glasses after immersion in SBF

### 4.4 CONCLUSIONS

In the present investigation, a comparative investigation was carried out on physico-mechanical and bioactive properties of zirconium dioxide substituted 1393 bioactive glasses. The following conclusions were drawn from this investigation. The XRD analysis of the bioactive glass before immersing into SBF showed the amorphous nature of the glass. FTIR reflectance spectra, pH behavior, XRD and SEM images indicate the formation of hydroxylapatite (HA) layer on the surface of the zirconium dioxide containing bioactive glasses after immersing in simulated body fluid (SBF). FTIR results showed the silicate network structure in prepared bioactive glass and increasing the zirconium dioxide content in 1393 bioactive glass increase the density, flexural strength, compressive strength, and microhardness. Hence, the present investigation clearly indicates that  $ZrO_2$  substituted bioactive glass would be potential biomaterials for biomedical applications.